Chapter

The “Natural Time” Method Used for the Potential Assessment for Strong Earthquakes in China Seismic Experimental Site

Shengfeng Zhang and Yongxian Zhang

Abstract

Due to the direct achieving for the state of stress or the strain along the earthquake fault which is quite essential in the assessment for the potential of strong earthquakes, the method of nowcasting earthquakes using the ‘natural time’ concept has been used in several locations worldwide and shown significant result. In this work, the Earthquake Potential Score (EPS) was determined using the nowcasting approach before several earthquake cases in the China Seismic Experimental Site (CSES) and analyze the consistency with the observation to evaluate its effectiveness. Firstly, with the importance of the data quality to this statistical method, we describe the background seismicity of the CSES area. Secondly, ergodicity research demonstrates the differences that exist in sub-regions such as Sichuan and the Yunnan region, mainly due to the simultaneous impact with the 2008 Wenchuan 8.0 earthquake. In the end, the strong earthquake potential prior to four earthquakes with magnitude larger than 6.0 was ultimately determined using the nowcasting method, which has EPS above 0.8. This may give support for the interpretation of EPS in earthquake nowcasting and will serve as a key reference for the ongoing development of this technology.

Keywords: China seismic experimental site (CSES), “natural time”, nowcasting method, earthquake potential

1. Introduction

The North-South Seismic Region in central China is one of the focal regions that pays special attention to decreasing the threat of earthquakes in China. A number of devastating earthquakes took place in this area, containing the 1920 Haiyuan M8.5 earthquake, the 1970 Tonghai M_S7.8 earthquake, the 2008 Wenchuan M_S8.0 earthquake, and 2013 Lushan M_S7.0 earthquake. This seismic zone was encircled by the Ordos block, the Sichuan Basin, and the Tibetan Plateau in the tectonic backdrop [1]. The Indian plate colliding with the Eurasia plate, which caused the Tibetan plateau to rise and expand, is represented by the region’s variation in crust thickness, which ranges from 30 to 46 km in the east to 46–74 km in the west [2]. There exist two experiment sites in history, one is the West-Yunnan Earthquake Prediction Experiment Site in 1980, and another is the National Experiment Site for Earthquake Monitoring and Forecast in 2014, have both been established there because of the region's reality [3]. Following the Regional Earthquake Likelihood Models (RELM) workshop, SCEC suggested that other regions take part in the testing process for various prediction models using religious assessment methodologies. The Collaboratory for the Study of Earthquake Predictability is offering this location as one of the first testing sites in China [4, 5].

The China Seismic Experimental Site (CSES) was launched on May 12, 2018 [6–8]. Given that CSES only covers the Chinese provinces of Sichuan and Yunnan, its geographic scope is less extensive than that of the field site before it. It builds on ideas from ecology and environmental science to propose Coordinated Distributed Experiments (CDEs), a novel collaborative research strategy that follows the design for CSES [9]. As CESE work has progressed in recent years, the concepts of retrospective and prospective [10], start and trial [7], planning and test [11], earthquake forecasting, and system design [12] have been revised. At the same time, the testing facility will be built in the CSES area as part of CSEP2.0, which was also announced in 2019 [13–17]. This study will provide an overview of seismicity analysis using historical and contemporary catalogs, the nowcasting experiment, and ergodicity feature, particularly for the potential assessment prior to strong events like August 3, 2014, Ludian M_S6.5 earthquake; October 7, 2014, Jinggu M_S6.6 earthquake; May 21, 2021, Yangbi M_S6.4 earthquake; and September 5, 2022, Luding M_S6.8 earthquake. **Figure 1** depicts the geographical distribution of earthquakes in the CSES area with a magnitude greater than 6.0 from 700 B.C. to A.D. 2022.

2. The earthquake catalog used

The earthquake catalog we utilized was integrated with the historical catalog for occurrences before 1970/01/01 and the contemporary catalog from 1970/01/01 to 2022/11/20 given by the China Earthquake Networks Center (CENC). **Figure 2** illustrates the capacity to record earthquake events in the CSES area, where ancient Chinese recording mentions some 8+ earthquakes, by varying the event number plot inside each magnitude bin and the magnitude-sequence number plot [18, 19]. As a consequence of the construction of the seismic station, and the disturbing occurrence of a few big earthquakes, the result indicates that there are certain peculiar time nodes that disclose the variation of monitoring capability in this area.

To obtain the completeness distribution of the modern earthquake catalog after 1970, many statistical methods based on the earthquake catalog [20] are usually used. **Figure 3** shows the assessment of the completeness state using the Best Combination method (Mc95-Mc90-Max curvature) [20], which reveals the temporal variation mainly depending on the development of observational facilities. The results for the catalog before 1970 give a completeness magnitude of around 5.0–6.0, however, there is a significant error since there are so few records, compared with that of the modern earthquake catalog. In general, the magnitude threshold of the historical earthquake catalog should be chosen as 4.0–4.5 to ensure the completeness level and enough sample size if a statistical algorithm would be used to analyze the sequence. For the catalog after 1970, 3.0–4.0 can be determined to be the completeness magnitude level [5]. On the other hand, strong earthquakes, such as the seismic sequence of Wenchuan 8.0 in 2008 and Lushan 7.0 in 2013, have a substantial influence on the catalog's

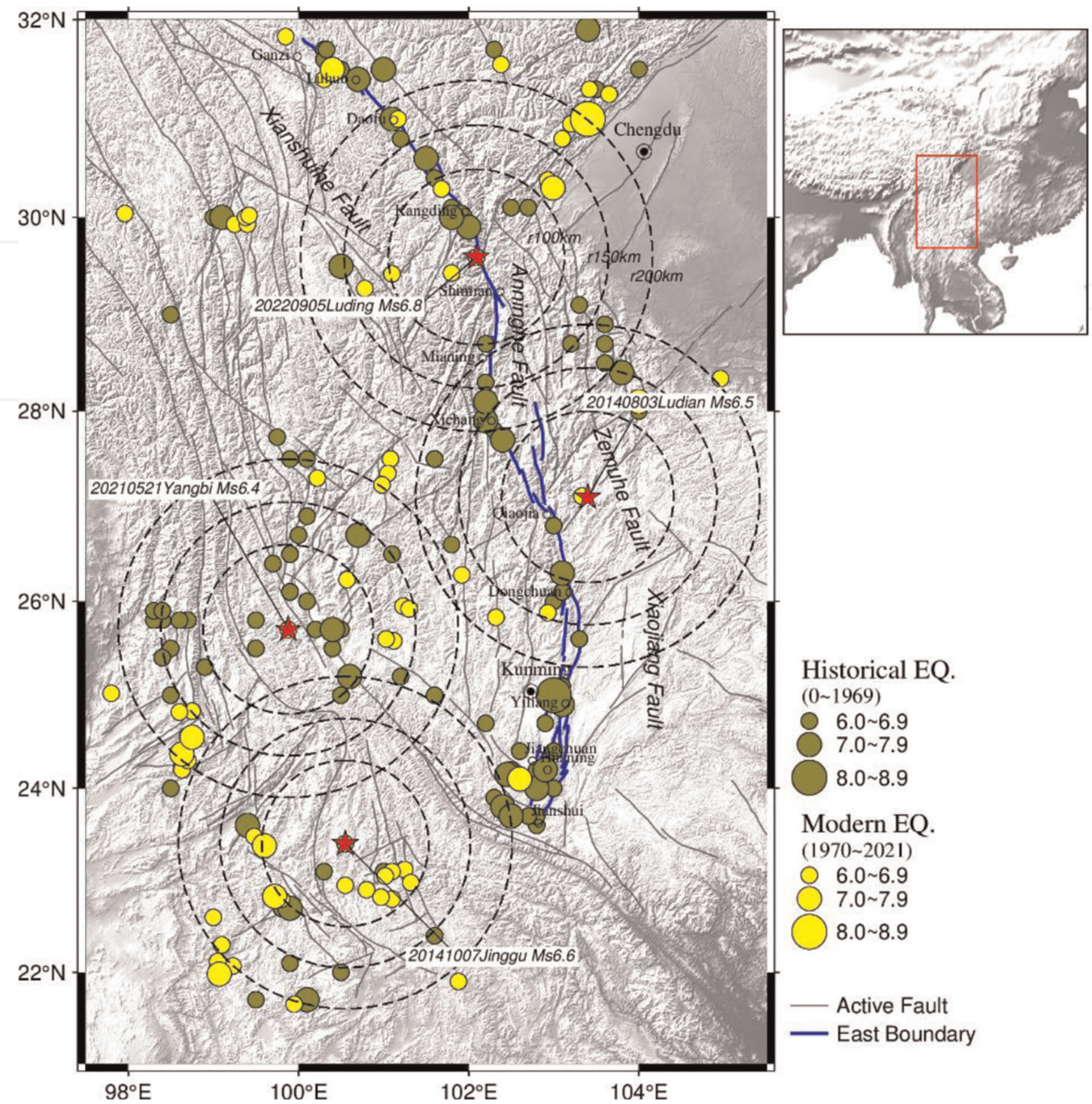

Figure 1.
Spatial distribution of earthquakes with magnitude above 6.0 for the period from 700 B.C. to A.D. 2022 in CSES region. The dots in dark yellow indicate the strong earthquakes up to 1970. Earthquakes that occurred since 1970/01/01, are shown in light yellow. The area being studied is shown in the indexing graphic at the upper right. The three dashed circles indicate the region with a radius of 100, 150, and 200 km, respectively, used in the nowcasting analysis. Center of these circles (the star in red) is the epicenter of the September 5, 2022, Luding M_S*6.8 earthquake; May 21, 2021, Yangbi* M_S*6.4 earthquake; October 7, 2014, Jinggu* M_S*6.6 earthquake; and August 3, 2014, Ludian* M_S*6.5 earthquake.*

completeness owing to observational limitations and regular seismological interpretation, which should be addressed in the future. The cut-off magnitude of 4.0 may be interpreted as the magnitude threshold in the following statistical models as a global estimate.

A "mixed" magnitude system is used in the earthquake catalog since 1970. The local type of magnitude (M_L) is utilized for events with magnitudes under 4.0. Surface wave type of magnitude (M_S) is utilized for earthquakes greater than magnitude 5.5. The change from M_L to M_S is not well defined for the events in between. Only "magnitude" is used in this research to indicate the size of events due to the magnitude uncertainty. The outcomes of the numerical calculations conducted in this chapter, such as the determination of the Earthquake Potential Score using the nowcasting technique, are unaffected by the magnitude uncertainty [21–24]. In line with Rundle's research [24], we used a threshold magnitude of 4.0 and a target magnitude of larger

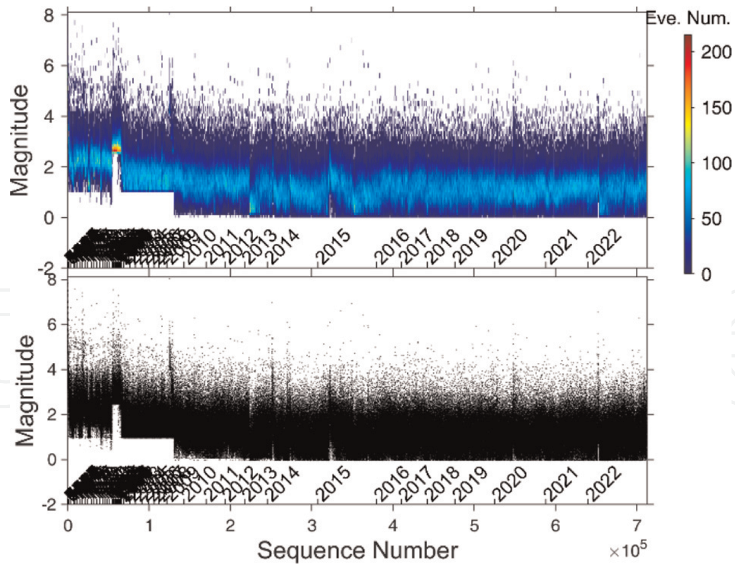

Figure 2.
Variation of event number within each magnitude bin (top) and the magnitude-sequence number plot (bottom) of the catalog of CSES region from 700 B.C. to A.D. 2022/11/20. In the event number plot, the number window of the x-axis is chosen as 500. The text above the x-axis shows the calendar time. In the magnitude-sequence plot, to avoid the difficulty to observe the little distribution of magnitude, a random of [−0.05, 0.05] is added into the fluctuation of the magnitude bin.

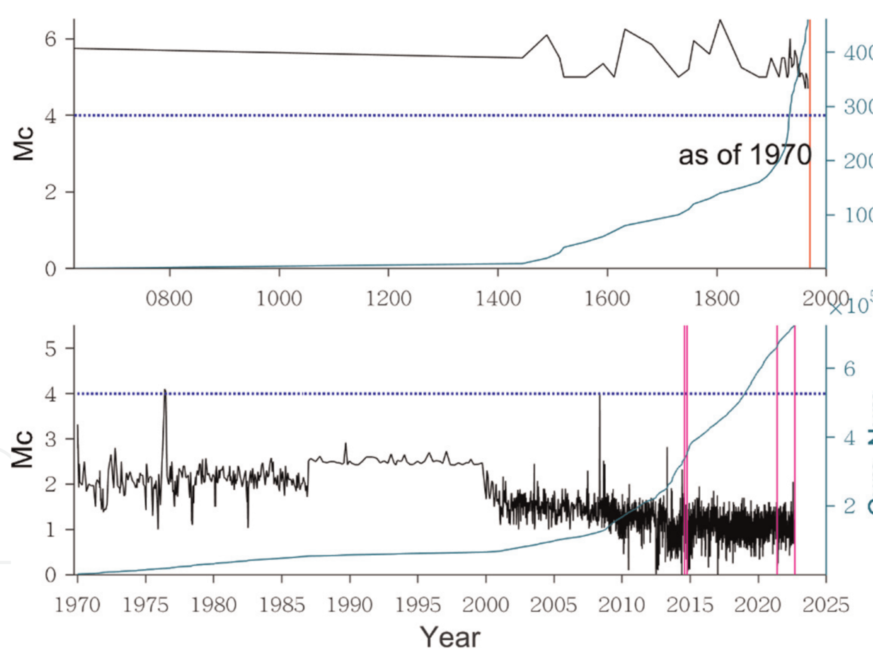

Figure 3.
Completeness magnitude and cumulative number analysis for the earthquake catalog of CSES. The above and bottom plots show the result of 700 B.C. to 1970 and 1970 to 2022/11/20. The black line in the plot indicates the completeness magnitude calculated using the Best Combination method (Mc95-Mc90-Max curvature) [20]. The blue lines show the cut-off magnitude level considering the global temporal variation of completeness magnitude. The dark green line shows the cumulative event number as the time. The vertical pure light red line marks the time of 1970/01/01, which separates the whole catalog into above and bottom plots. The vertical purplish red lines mark the occurrence time of four target strong earthquakes in this study.

than 6.0 in our investigation. However, for alternative methods that evaluate not only the frequency of earthquakes but also their size, concerns of magnitude transition, and magnitude uncertainty must be considered.

3. Ergodicity analysis

Some studies have suggested that driven mean-field systems may often display significant ergodic behavior. Moreover, Egolf [25] and Tiampo et al. [26, 27] gave the study that statistically stationary models have the propensity to live in a set of physical states resembling equilibrium. Large events, however, usually reveal the potential to temporarily throw the study target out of balance before it returns to its original state. We apply the method of Tiampo et al. [27, 28] to quantify the base level of heterogeneity and, as a consequence, the predictability of target earthquakes due to the temporal complexity of the small events in the CSES zone, as shown in **Figure 2**. According to the method of Thirumalai et al. [29] and Thirumalai and Mountain [30], it is possible to evaluate ergodicity behavior generally using the Thirumalai-Mountain plot (the TM metric). Originally, the TM metrics may be used to assess effective ergodicity or the discrepancy between the time average of a quantity, commonly associated with energy, at every cell or grid of the system. A simple statistical algorithm, such as the pattern of Informatics (PI) algorithm, may be determined by the TM metrics, not by looking at energy levels, but rather at the frequency of observations [31].

The beginning of the earthquake catalog corresponds to the starting time $t = 0$ and the function $TM_n(t)$, which is computed in the analysis at extensive time t, is defined as

$$TM_n(t) = \frac{1}{L}\sum_{i=1}^{L}\left[n_i(t) - \overline{n}(t)\right]^2 \tag{1}$$

$n_i(t)$ is the count of events located within the ith grid in the period of $0 \sim t$, L is the number of grids in the spatial range, and $\overline{n}(t)$ is the average count of events across all cells during the period $0 \sim t$,

$$n_i(t) = \frac{1}{t}\int_0^t n_i\left(t'\right)dt' \tag{2}$$

$$\overline{n}(t) = \frac{1}{L}\sum_{i}^{L} n_i(t) \tag{3}$$

Tiampo et al. [27, 28] found that, as shown in Eq. (1), all grids or cells in the system are comparable in properties, especially in the case of physical characteristics, and the deviation of the average quantity in temporal from grouped mean number is diminishing. The statement states that if the system exhibits the behavior of "effective ergodic" over an extended length of time, time t will have a direct relationship with the function $1/TM$. With a grid size of $0.2° \times 0.2°$ and a cut-off magnitude of 3.0, **Figure 4** depicts the $1/TM$ metrics of the seismicity from 1970 to 2022 in the CSES area, Sichuan and Yunnan portions. Before 1980, we can observe from the instance of including and not containing the Wenchuan aftershocks that both the Yunnan and Sichuan regions had weak ergodicity and display unique ergodic tendencies. After accounting for changes in the earthquake catalog caused by technology and network problems, Tiampo et al. [27, 28] found that natural seismicity exhibited ergodicity. In this study, when taking into account the condition of China's seismic networks, the regionalized aspects of seismological observation and artificial processing can be responsible for the behavior of ergodicity. The seismicity across the entire CSES area and two sub-regions exhibits excellent ergodicity since about 1980. Taking the Sichuan region as an example, where the Wenchuan earthquake's aftershocks mostly contributed to the disruption of the 1/*TM* metric in 2008.

4. Nowcasting method

The term "nowcast" has existed for a very long period in the fields of meteorology and economics. It has now been applied to a variety of fields, including stock market trend forecasting, displaying the cloud movement in real-time, and application in hazard assessment of strong earthquakes under the name "Nowcasting Earthquakes" [21–24]. In contrast to "forecasting," which was usually used to produce a probabilistic estimate of future events in the seismic cycle, it often focuses on the identification of the current state of a system using indirect approaches. In the field of seismology research, this strategy has traditionally been utilized in regions with a long history of earthquake records and reasonably high seismic activity. The technique has recently been used to estimate the seismic risk for a number of places, including California [24, 32], Tokyo [22], the Himalayas [33], and New Zealand [34], among others. To compute the Earthquake Potential Score (EPS), the nowcasting technique made use of the frequency of little events that occurred between larger ones in the same or a nearby study location with a similar dynamic development history. The magnitude threshold for small events should be chosen so that all events in the database are a completeness sequence. The key benefit of this technique is that it is easier to use than the direct method of hazard identification in earthquake forecasting and prediction which seems to be difficult to implement in reality.

The study of Varotsos et al. [35–37] suggested that the "natural time" in the nowcasting method is calculated by counting the number of little events that have occurred in a studied location since the previous strong earthquake. Target events are indicated by M_λ, whereas little events are indicated by M_σ (4.0), which accounts for the completeness of the historical and present catalog. The Gutenberg-Richter magnitude-frequency relationship may characterize the average frequency of small events larger than M_σ but with magnitude under M_λ [38]. The relation of Gutenberg-Richter relation is used here to obtain the average count of events larger than M,

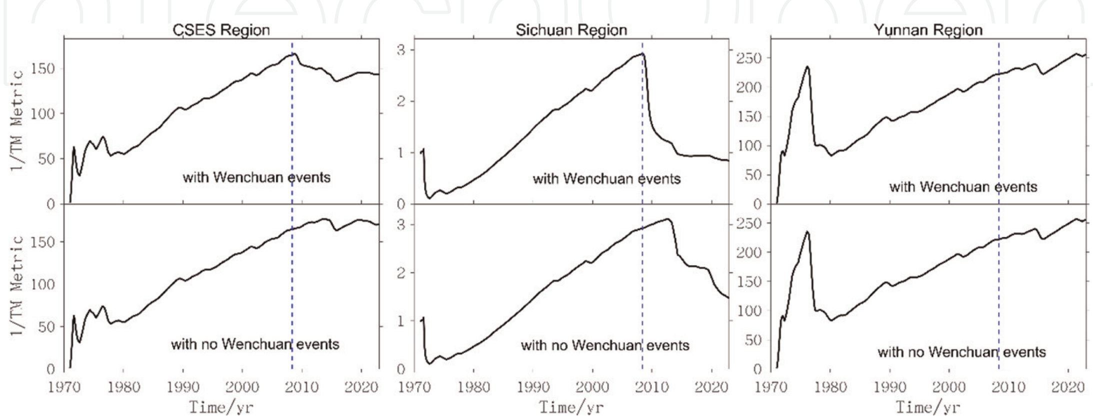

Figure 4.
The 1/TM metric indicates the seismic ergodicity in the CSES region. The left, middle and right plots show the entire CSES, Sichuan, and Yunnan region, respectively. The top and bottom show the case computed with and without aftershocks of the Wenchuan 8.0 earthquake. The vertical dashed lines reflect the occurrence time of the 2008 Wenchuan earthquake.

$$N_{avg} = 10^a 10^{-bM} \tag{4}$$

where b is normally close to 1, a value indicates the background level of seismicity.

If we use N_σ to represent the average number of little events more than M_σ, N_λ the mean frequency of events greater than M_λ, respectively,

$$N_\sigma = 10^a 10^{-bM_\sigma} \tag{5}$$

$$N_\lambda = 10^a 10^{-bM_\lambda} \tag{6}$$

then we can determine how many little earthquakes there are on average between large earthquakes:

$$N = \frac{N_\sigma - N_\lambda}{N_\lambda} = 10^{b(M_\lambda - M_\sigma)} - 1 \tag{7}$$

N in this case is independent of a value.

By calculating the cumulative distribution function (CDF) with the help of small events with magnitudes in $[M_\sigma, M_\lambda]$, the mathematical process of nowcasting computation may be stated in terms of the potential for massive earthquakes (target events). The probability density function (PDF) and cumulative distribution function of small events with magnitudes in $[M_\sigma, M_\lambda]$ within every larger cycle are calculated using the scientific mathematical approach of Bevington and Robinson [39]. The current CDF may be calculated using the present frequency of little events, $n(t)$, where t is the time from the most recent large event. The earthquake potential score (EPS) at time t may be used to define this value:

$$\text{EPS} = p[n \leq n(t)] \tag{8}$$

The likelihood that the next significant earthquake in our research zone with a magnitude larger than M_λ will occur is determined by the EPS. According to Eqs. (7) and (8), the EPS value will rise over time after the most recent significant earthquake before abruptly returning to zero when the next significant earthquake strikes. It will then begin to rise once again until the next significant event happens. Therefore, in this process, there is just one straightforward method of interpreting the earthquake data throughout the whole procedure, with no fitting calculations for the model parameters. This approach may be used for both a broad seismic zone and a small area, such as a regional area of a city, as there is no connection between the EPS definition and the rate of earthquakes in the area under study.

5. Earthquake potential before target earthquakes

In the previous study as Rundle et al. [24], a circle area around the city was usually used when we want to assess the potential to occur next strong earthquake, and the seismicity in a relatively large region will be selected to build the background database to describe the statistical characteristic. Alternately, here we choose a circle area around the epicenter of four earthquakes, that is, August 3, 2014, Ludian M_S6.5 earthquake; October 7, 2014, Jinggu M_S6.6 earthquake; May 21, 2021, Yangbi M_S6.4 earthquake; and September 5, 2022, Luding M_S6.8 earthquake, to assess the potential before the occurrence of these four events, and used the seismicity of CSES as the large region to build the background database. We investigate circular regions with radii of 100, 150, and 200 km to test the analysis's resilience to parameter fluctuation. **Figure 5** shows the EPS result (case of radii 200 km) calculated using the nowcasting technique for these four events. For instance, **Figure 5a** shows that since the previous significant event with a magnitude over 6.8 on 2013/4/20, there have been 113 small events within 200 km of the epicenter of the Luding M_S6.8 earthquake, and the EPS value has reached 81%. The EPS value for the remaining three earthquakes approaches 98, 87, and 88%, respectively, according to **Figure 5b–d**. **Table 1** lists the results obtained using various radii. We can observe that the EPS was high but did not reach 100% prior to the occurrence of these four events.

As a result of the big events' ability to segregate smaller events or samples, the amount of larger events will have an impact on how smoothly the EPS curve behaves in each plot. Even yet, the outcome of EPS results before these earthquakes might still indicate a rather high likelihood of subsequent large earthquakes. How to comprehend the high EPS with the possibility of the next large earthquake is one issue that has persisted from earlier investigations. Because the EPS is high in this research but does not reach 100%, it is not required to wait for the EPS to reach 100% before the next

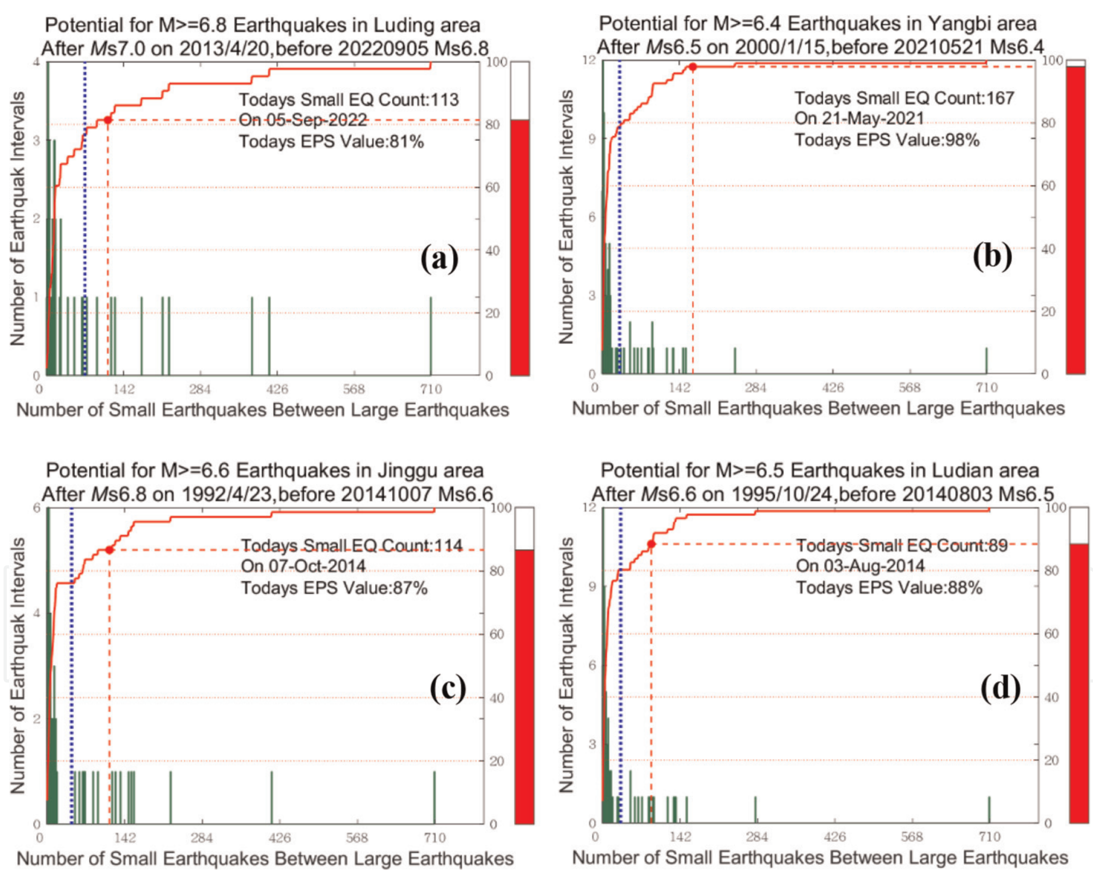

Figure 5.
The nowcasting approach was used to compute the Earthquake Potential Score (EPS) up to the occurrence of certain target events in the CSES zone. (a) Assessment for $M \geq 6.8$ *before the occurrence of Luding* $M_S6.8$ *on September 20, 2022; (b) assessment for* $M \geq 6.4$ *before the occurrence of Yangbi* $M_S6.4$ *on May 21, 2021; (c) assessment for* $M \geq 6.6$ *before the occurrence of Jinggu* $M_S6.6$ *on October 7, 2014; and (d) assessment for* $M \geq 6.5$ *before the occurrence of Ludian* $M_S6.5$ *on August 3, 2014. The green bars in each plot show the number of small events (*$M_\sigma \geq 4.0$*) in the interval of strong earthquakes. The red curve shows the CDF of earthquake intervals varied with the number of small events. The red points on the curve show the current EPS value since the occurrence of the last strong earthquake and the EPS state is shown on the right with a "hot bar." The dashed vertical line in blue indicates the mean count of small events in the intervals according to the statistical analysis for the database.*

Target events	M_λ	EPS result		
		R = 100 km	R = 150 km	R = 200 km
2014-08-03 Ludian M_S6.5	6.5	86%	85%	88%
2014-10-07 Jinggu M_S6.6	6.6	84%	91%	87%
2021-05-21 Yangbi M_S6.4	6.4	96%	96%	98%
2022-09-05 Luding M_S6.8	6.8	73%	79%	81%

Table 1.
EPS before different target events with different circular regions with radii R.

significant earthquake occurs. When interpreting the EPS using the nowcasting technique, it is useful to keep in mind that the area under investigation is nearing another large earthquake when the EPS is rising high.

6. Summary and discussion

To characterize the fundamental aspects of seismicity, we examined the earthquake catalog in the CSES area. We determine the cut-off magnitude with 4.0 in this study according to the temporal distribution of completeness magnitude and the features of the database containing historical and modern earthquake catalog. Further research showed that ergodicity persists over the vast majority of the time from 1980 to the present, presenting evidence for the meta-stable equilibrium hypotheses. The clustering of Wenchuan aftershocks makes the Yunnan area's ergodicity superior to that of Sichuan's, which means Sichuan's influence on the ergodicity of the whole CSES is dominant. Four earthquakes, that is, August 3, 2014, Ludian M_S6.5 earthquake; October 7, 2014, Jinggu M_S6.6 earthquake; May 21, 2021, Yangbi M_S6.4 earthquake; and September 5, 2022, Luding M_S6.8 earthquake, whose potential was assessed using the nowcasting approach. To consider the influence of chosen parameters, we select radii 100, 150, and 200 km in the nowcasting method to analyze the EPS before the occurrence time of them. The outcome indicates that the EPS is high but does not achieve 100%, suggesting a scientific interpretation of the EPS when the next significant earthquake in this area is about to occur.

It was revealed in this research that the nowcasting approach may be used to define the earthquake potential after the geographical area has been identified. How far the prediction window from now can be given by this approach, in reality, is one of the concerns that need further debate. For this problem, combining the Annual Consultation Conference in China with the nowcasting approach may be a viable option, which may determine its relevance to the particular earthquake work in different locations. Previous research has shown that such yearly forecasts perform better than random guesses [40]. However, for the nowcasting technique, the present EPS is a crucial and fundamental piece of knowledge when we want to understand the potential in the sphere of catastrophe preparation.

Acknowledgements

We are grateful to Prof. Wu Zhongliang in the Institute of Earthquake Forecasting, China Earthquake Administration, Prof. John B. Rundle in UC Davis, and Jiang Changsheng in Institute of Geophysics, China Earthquake Administration for their assistance and guidance with the nowcasting method and earthquake catalog analysis. The earthquake catalog utilized in this investigation was given by the China Earthquake Networks Center (CENC). This study is also sponsored by the National Natural Science Foundation of China (42004038, U2039207), the National Key Research and Development Program of China (2018YFE0109700) and the Special Fund of the Institute of Earthquake Forecasting, China Earthquake Administration (CEAIEF2022030206).

Author details

Shengfeng Zhang* and Yongxian Zhang
Institute of Earthquake Forecasting, China Earthquake Administration, Beijing, China

*Address all correspondence to: 085012104@163.com

References

[1] Zhang PZ, Deng QD, Zhang GM, Ma J, Gan WJ, Min W, et al. Active tectonic blocks and strong earthquakes in the continent of China. Science in China Series D: Earth Sciences. 2003;**46**: 13-24. DOI: 10.1360/03dz0002

[2] Li SL, Mooney WD, Fan JC. Crustal structure of mainland China from deep seismic sounding data. Tectonophysics. 2006;**420**:239-252. DOI: 10.1016/j.tecto.2006.01.026

[3] Sun QZ, Wu SG. Development of the Earthquake Monitoring and Prediction in China during 1966~2006. Beijing: Seismological Press; 2007

[4] Jordan TH. Earthquake predictability, brick by brick. Seismological Research Letters. 2006;**77**:3-6. DOI: 10.1785/gssrl.77.1.3

[5] Mignan A, Jiang CS, Zechar JD, Wiemer S, Wu ZL, Huang Z. Completeness of the Mainland China earthquake catalog and implications for the setup of the China Earthquake Forecast Testing Center. Bulletin of the Seismological Society of America. 2013; **103**:845-859. DOI: 10.1785/0120120052

[6] Wu ZL. Seismic experimental sites: Challenges and opportunities. Journal of Geological Society of India. 2020;**95**: 113-116. DOI: 10.1007/s12594-020-1400-9

[7] Wu ZL, Li Q, Zhang XD, Li L, Tang Y, Che S, et al. China seismic experimental site (CSES): Start and trial. Reviews of Geophysics and Planetary Physics. 2021;**52**(6):675-678. DOI: 10.19975/j.dqyxx.2021-012

[8] Wu ZL, Zhang XD, Sun K. China seismic experiment site: Scientific challenges. Acta Geologica Sinica-English Edition. 2019;**93**:273-273. DOI: 10.1111/1755-6724.14084

[9] Wu ZL, Zhang Y, Li JW. Coordinated distributed experiments (CDEs) applied to earthquake forecast test sites. In: Li Y-G, editor. Earthquake and Disaster Risk: Decade Retrospective of the Wenchuan Earthquake. Singapore: Higher Education Press and Springer Nature Singapore Pte Ltd.; 2019. pp. 107-115

[10] Wu ZL, Ding ZF, Zhang XD, Li L, Shao ZG, Li Y, et al. China seismic experimental site: Retrospective and prospective. Reviews of Geophysics and Planetary Physics. 2021;**52**(2):234-238. DOI: 10.19975/j.dqyxx.2020-023

[11] Wu ZL, Wang L, Che S, Li L, Zhang XD, Shao ZG, et al. China seismic experimental site (CSES): Planning and test. Reviews of Geophysics and Planetary Physics. 2021;**52**(3):348-352. DOI: 10.19975/j.dqyxx.2021-010

[12] Wu ZL, Wang L, Li L, Zhang XD, Shao ZG, Li Y, et al. China seismic experimental site (CSES): Earthquake forecast and system design. Reviews of Geophysics and Planetary Physics. 2021; **52**(6):679-683. DOI: 10.19975/j.dqyxx.2021-028

[13] Michael AJ, Werner MJ. Preface to the focus section on the Collaboratory for the Study of Earthquake Predictability (CSEP): New results and future directions. Seismological Research Letters. 2018;**89**:1226-1228. DOI: 10.1785/0220180161

[14] Savran WH, Maechling PJ, Werner MJ, Jordan TH, Schorlemmer D, Rhoades DA, et al. The Collaboratory for the Study of Earthquake Predictability

version 2.0 (CSEP2.0): New capabilities in earthquake forecasting and testing. In: Poster Presentation at 2018 SCEC Annual Meeting. Los Angeles. 2018

[15] Zhang YX, Wu ZL, Zhang XD, Yu HZ, Zhang S, Zhang XT, et al. CSEP2 from China perspective. In: Poster Presentation at 2019 SCEC Annual Meeting. Los Angeles. 2019

[16] Zhang SF, Zhang YX. Collaborratory for the Study of Earthquake Predictability working philosophy and ten years' achievements of CSEP1.0. Earth. 2021;**41**(4):203-217. DOI: 10.12196/j.issn.10003274.2021.04.016

[17] Zhang YX, Wu ZL, Zhang XT, Li G. Annual earthquake potential consultation: A real forward prediction test in China. In: Li Y-G, editor. Earthquake and Disaster Risk: Decade Retrospective of the Wenchuan Earthquake. Singapore: Higher Education Press and Springer Nature Singapore Pte Ltd.; 2019. pp. 117-134. DOI: 10.1007/978-981-13-1085-0_5

[18] Department of Earthquake Disaster Prevention of the State Seismological Bureau. The Catalogue of Chinese Historical Strong Earthquakes. Beijing: Seismological Press; 1995

[19] Department of Earthquake Disaster Prevention of the China Earthquake Administration. The Catalogue of Chinese Modern Earthquakes. Beijing: China Science and Technology Press; 1999

[20] Woessner J, Wiemer S. Assessing the quality of earthquake catalogues: Estimating the magnitude of completeness and its uncertainty. Bulletin of the Seismological Society of America. 2005;**95**:684-698. DOI: 10.1785/0120040007

[21] Rundle JB, Luginbuhl M, Giguere A, Turcotte DL. Natural time, nowcasting and the physics of earthquakes: Estimation of seismic risk to global megacities. Pure and Applied Geophysics. 2017;**175**:647-660. DOI: 10.1007/s00024-017-1720-x

[22] Rundle JB, Luginbuhl M, Giguere A, Turcotte DL. Natural time, nowcasting and the physics of earthquakes: Estimation of risk to global megacities. Pure and Applied Geophysics. 2018;**175**:647-660. DOI: 10.1007/s00024-017-1720-x

[23] Rundle JB, Luginbuhl M, Giguere A, Turcotte DL. Natural Time, Nowcasting and the Physics of Earthquakes: Estimation of Seismic Risk to Global Megacities. In: Williams C, Peng Z, Zhang Y, Fukuyama E, Goebel T, Yoder M, editors. Earthquakes and Multi-hazards Around the Pacific Rim, Vol. II. Pageoph Topical Volumes. Cham: Birkhäuser. 2019. DOI: 10.1007/978-3-319-92297-3_10

[24] Rundle JB, Turcotte DL, Donnellan A, Grant Ludwig L, Luginbuhl M, Gong G. Nowcasting earthquakes. Earth and Space Science. 2016;**3**:480-486. DOI: 10.1002/2016ea000185

[25] Egolf DA. Equilibrium regained: From nonequilibrium chaos to statistical mechanics. Science. 2000;**287**(5450):101-104. DOI: 10.1126/science.287.5450.101

[26] Tiampo KF, Rundle JB, Klein W, Martins JSS, Ferguson CD. Ergodic dynamics in a natural threshold system. Physical Review Letters. 2003;**91**(23):238501. DOI: 10.1103/PhysRevLett.91.238501

[27] Tiampo KF, Rundle JB, Klein W, Holliday J, Sá Martins JS, Ferguson CD.

Ergodicity in natural earthquake fault networks. Physical Review E. 2007;**75**: 066107. DOI: 10.1103/PhysRevE. 75.066107

[28] Tiampo KF, Rundle JB, Klein W, Martins JSS. Ergodicity in natural fault systems. Pure and Applied Geophysics. 2004;**161**:1957-1968. DOI: 10.1007/ s00024-004-2542-1

[29] Thirumalai D, Mountain RD, Kirkpatrick TR. Ergodic behavior in supercooled liquids and in glasses. Physical Review A. 1989;**39**:3563-3574. DOI: 10.1103/PhysRevA.39.3563

[30] Thirumalai D, Mountain RD. Activated dynamics, loss of ergodicity, and transport in supercooled liquids. Physical Review E. 1993;**47**:479-489. DOI: 10.1103/PhysRevE.47.479

[31] Tiampo KF, Rundle JB, McGinnis S, Gross SJ, Klein W. Mean-field threshold systems and phase dynamics: An application to earthquake fault systems. Europhysics Letters. 2002;**60**(3):481-487. DOI: 10.1209/epl/i2002-00289-y

[32] Rundle JB, Donnellan A. Nowcasting earthquakes in southern California with machine learning: Bursts, swarms, and aftershocks may be related to levels of regional tectonic stress. Earth and Space Science. 2020;**7**:e2020. DOI: 10.1029/ 2020EA001097

[33] Pasari S, Sharma Y. Contemporary earthquake hazards in the west-northwest Himalaya: A statistical perspective through natural times. Seismological Research Letters. 2020;**91**: 3358-3369. DOI: 10.1785/0220200104

[34] Pasari S, Neha. Nowcasting-based earthquake hazard estimation at major cities in New Zealand. Pure and Applied Geophysics. 2022;**179**:1597-1612. DOI: 10.1007/s00024-022-03021-z

[35] Varotsos PA, Sarlis NV, Skordas ES. Long-range correlations in the electric signals that precede rupture. Physical Review E. 2002;**66**:011902. DOI: 10.1103/PhysRevE.66.011902

[36] Varotsos PA, Sarlis NV, Skordas ES. Natural Time Analysis: The New View of Time. Berlin: Springer; 2011

[37] Varotsos PA, Sarlis NV, Tanaka HK, Skordas ES. Some properties of the entropy in the natural time. Physical Review E. 2005;**71**:032102. DOI: 10.1103/ PhysRevE.71.032102

[38] Scholz CH. The Mechanics of Earthquakes Faulting. Cambridge, UK: Cambridge Univ. Press; 1990

[39] Bevington PR, Robinson DK. Data Reduction and Error Analysis for the Physical Sciences. 3rd ed. Boston (Mass.): McGraw-Hill; 2003

[40] Shi YL, Liu J, Zhang GM. An evaluation of Chinese annual earthquake predictions, 1990-1998. Journal of Applied Probability. 2001;**38A**:222-231. DOI: 10.1239/jap/1085496604